Optimal Control of 3.5 MW Solar Hybrid Power Plant of Joseph SarwuanTarka University Makurdi Benue State, Nigeria

ABSTRACT

~~Operation~~ The operationof ~~power-generating~~ power-generating plants becomes complex when two or more sources of power are combined. The decision of which source should take priority of load demand at various intervals requires sensitive control approaches. The Joseph SarwuanTarka University Makurdi (JOSTUM) 3.5 Mega Watts Solar Hybrid Power Plant (SHPP) ~~which~~ has one renewable system; photovoltaic (PV) array, one energy storage system; battery bank, and one ~~back-up~~ backup system; diesel generator (DG), power conversion devices; Photovoltaic inverter (PVI), power conditioning system (PCS), and switchgears was modelled and simulated. ~~Emphasis~~ The emphasisof the research is to obtain a control technique, which when applied to the PVI would improve the power produced from the PV array system. For a PV module to harvest the maximum amount of solar energy and simultaneously attain higher efficiency, PV systems must be operated at their maximum power point (MPP) under partially shaded conditions (PSC), varying irradiances, and temperature. Maximum power point tracking (MPPT) methods are capable of guaranteeing MPP under varying climatic conditions. A control scheme is proposed using Whale Optimization Algorithm (WOA)-based MPPT control technique in order to improve the output power of the PV array. The output of the existing system from the PV array is about 1,800 kW, but when the WOA-based MPPT control technique is applied, an output of about 2,800 kW is produced. To validate the choice of the proposed technique, perturb and observe (P and O) algorithm for MPPT was tested on the system, which generated a mean power of 2,300 kW. The results proved that the proposed technique has an efficiency of 55.56% greater than the existing and P and O MPPT-based algorithm, which has 27.78%. The simulation ~~Simulation~~ was accomplished via MATLAB/Simulink.

Keywords:*Photovoltaic inverter, power conditioning system, maximum power point tracking, perturb, and observe, whale optimization algorithm.*

1. INTRODUCTION

A typical Hybrid Renewable Energy System (HRES) consists of two or more energy sources; these sources may include, wind generators, solar photovoltaic cells with energy storage, etcetera. These systems are attractive because the individual sources could complement one another to provide more reliable power to the user than a single-source system. In order to ensure ~~the~~ better conditions for continuity of power delivery to the local loads, it is essential to make Wind Turbine Generators (WTGs), diesel generators (DG), and Photovoltaic (PV) systems compatible with additional energy storage systems. With the greater incorporation of renewable electricity generation like WTGs, DGs, and solar PV power into the existing grids, research efforts must be devoted to ~~formulate~~ formulatinggeneration scheduling problems, taking into account the intrinsic variability characteristics of these renewable energy resources. Joseph Sarwuan Tarka University (formally, University of Agriculture)Makurdi (JOSTUM) 3.5MW Solar Hybrid Power Plant (SHPP) comprises three (3) ~~parallel-connected~~ parallel-connected distributed resources (DGs, PV cells, and batteries) with electronically controlled strategies which are capable of operating both on islanded and ~~grid-connected~~ grid-connected mode. The SHPP based on renewable energy sources is the cost-effective option for solving the power supply problem in the university and could also be used to solve similar power problems in remote areas that are located far from grids. In this research, the DGs, PV cells, and batteries are used to design the islanded ~~micro-grid~~microgrid for providing the needed electricity. ~~Cost effectiveness~~ Cost-effectiveness, efficiency, and system reliability are the major factors considered in order to achieve better power management and control.

A new swarm-based optimization algorithm inspired by the hunting behaviour of humpback whales was performed. The proposed method, Whale Optimization Algorithm (WOA), included three operators to stimulate the search for prey, encircling prey, and bubble-net foraging behaviour of humpback whales. The WOA is found to be competitive with other state-of-the-art meta-heuristic methods and has proffered solutions to most engineering problems, among which is the solving of the optimal power flow problem [1]. WOA has been used to optimally design the Proportional Integral and Derivative (PID) controllers in ~~an~~ Automatic Generation Control (AGC) loops of multi-area interconnected modern power systems including the Renewable Energy System (RES). Design variables used include the proportional gain kp, the integral gain ki, the derivative gain kd, and the derivative filter coefficient N [2]. Analysis and simulation studies of complex HRES ~~was~~ wereperformed on a system consisting of a wind turbine with a Permanent Magnet Synchronous Generator (PMSG), photovoltaic panels, and battery energy storage. ~~Control~~ The controlalgorithm of PMSG with machine-side converter was based on rotor field-oriented control, considering the Traffic Sign Recognition (TSR) algorithm of MPPT. The research solved an Optimal Power Flow (OPF) considering wind–solar–storage hybrid generation system [3]. WOA was used to determine the optimal DG sizing of renewable resources for loss reduction in distribution systems. The WOA was evaluated on IEEE 15, 33, 69, and 85-bus test systems. WOA, a novel meta-heuristic algorithm, was used to determine the optimal DG size. Publications on multi-objective optimal power flow for a thermal-wind-solar power system to solve a novel Multi-Objective Optimal Power Flow (MO-OPF) problem for a hybrid power system consisting the thermal generators, Wind Energy Generators (WEGs), and solar PV units with Battery Energy Storage System (BESS), in which three objective functions, i.e., total generation cost, transmission losses, and voltage stability enhancement index were considered and optimized simultaneously using a modified IEEE 30 bus [4, 5, 6]. An optimal power flow control of a hybrid renewable energy system with energy storage was proposed [7]. The authors proposed an optimal control technique for power flow control of Hybrid Renewable Energy Systems (HRESs) like a combined photovoltaic and wind turbine system with energy storage. The proposed optimal control technique was a joint execution of both the WOA and the Artificial Neural Network (ANN). The ANN learning process was enhanced

by utilizing the WOA optimization process with respect to the minimum error objective function and named ~~as~~ WOANN. Whale optimization algorithms-based PI controllers of STATCOM for renewable hybrid power system was carried out [8]. The study introduced WOA-based PI controllers for controlling STAT-COM. This WOA-PI controller of STATCOM was applied for a renewable hybrid system to improve the performance of the entire system [8]. Implementation of the Perturb and Observe (P and O)-based MPPT algorithm for the photovoltaic system was studied. The system consisted of a PV panel, DC-DC boost converter controlled by an Arduino microcontroller-based unit, and a resistive load. The results proved that P and O MPPT-based controller increases the output power of PV modules/array, which equally increases the system efficiency. WOA-based MPPT controller to track the maximum amount of output power from a PV array was also performed. The study experimented with how to track the maximum power at variable climatic and Partial Shaded Conditions (PSC). The proposed technique proved to possess a superior fit in terms of accuracy and tracking speed [9, 10]. Highlights on the planning and installation of 3.5 Megawatts of~~f~~ grid SHPP were ~~as~~ made [11]. The procedure for planning and installation was clearly elaborated. According to the authors, poly-crystalline PV modules, Valve Regulated Lead-Acid (VRLA) batteries, DGs, PVIs, PCSs, step-up transformers, and switch gears were installed. The system outputted maximum power of 2.5 MW, minimum power of 1.75 MW while load demand stood at 850 kW and 350 kW for maximum and minimum demands, respectively.

This work would focus basically on the modelling, simulation, and optimization of the JOSTUM 3.5 MW SHPP. The optimization shall be achieved by employing WOA. All analyses shall be done using MATLAB/Simulink software (version 2018b).

2. MATERIALS FOR CASE STUDY SIMULATION

This section captures materials employed for the modelling, simulation, and optimization of the JOSTUM 3.5 MW solar hybrid power plant (SHPP).

2.1 Overview of JOSTUM 3.5 MW Solar Hybrid Power Plant (SHPP)

The JOSTUM 3.5 MW SHPP consists of a PV array, an energy storage system (ESS), DGs, PVI, PCS, and switchgears. The PV array is made up of 607 parallel strings and 20 series connected strings, respectively. There are eight strings of ~~battery~~ batteries in three battery bank rooms, each string contains 1,098 batteries. The plant has three DGs connected in parallel. Power generated by each of the units is connected to the low voltage side of the step-up transformers. The secondary side of the step-up transformers of the various units ~~are~~ is linked to an 11 kV bus. Figure 1 depicts the ~~single line~~ single-line diagram of the JOSTUM 3.5 MW SHPP.

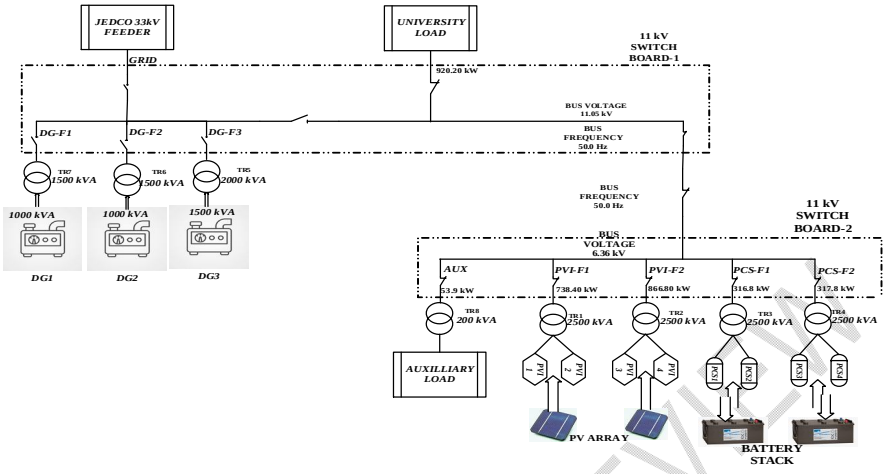

Figure 1: Single Line Diagram of JOSTUM 3.5 MW SHPP

2.2 Simulink Model Development of JOSTUM 3.5 MW SHPP

The modelling of the SHPP was achieved using MATLAB/Simulink. Some of the major systems that form the Simulink model of the system include;PV array (modules), batteries, diesel generators, PVIs, PCSs, transformers, and switchgears, respectively.

2.3 Photovoltaic (PV) Module

The photovoltaic module is modelled in MATLAB/Simulink using the PV array block, which implements a PV array built of series and parallel connected PV modules. It allows modelling a variety of pre-set PV modules available from the national renewable energy laboratory (NREL) system advisor model as well as a user-defined PV module. The PV array block has two inputs that allow the supply of varying solar irradiance (input$I_r (W/m^2)$) and temperature (input T in degrees Celsius) data. The Simulink block of the photovoltaic module is shown in Figure 2.

Figure 2: Simulink block of a Solar Photovoltaic Module

The positive (+) and negative (-) terminals represent the connection point through which the DC link is connected. The port marked “m” represents the output terminal of the block.

2.4 Photovoltaic Generating Unit (PVGU)

The photovoltaic modules are laid in tables; one table contains 20 modules in series, and two tables are connected in parallel form a string. Ten strings are fed to one string combiner box (SCB), the plant has a total number of 607 parallel strings and 20 series connected modules per string. Thirty-two (32) SCBs feed the entire plant. These SCBs are connected to the PVIs where power conversion from DC to AC at the PVGU takes place. Eight units of SCBs are connected to feed one PVI. The entire plant has four PVIs. Two PVIs feed one 2.5 MVA step-up transformer, which steps up the voltage to 11 kV. The 11 kV bus feeds the

local loads and the auxiliary unit. Due to the intrinsic variability nature of the sun during cloudy periods, this source is not always reliable, hence the need for having two or more generating units in a renewable energy system. The installed Energy Management System (EMS) incorporates the battery or DG at such periods for backup and the operation of the plant remains continuous. Theparameter dialogue box which enables the configuration of the PV array in MATLAB/Simulink is shown in Ffigure 3.

$$P_{PVGU}(t) = P_{PVI(1)} + P_{PVI(2)} + P_{PVI(3)} + P_{PVI(4)} \quad (1)$$

whereWhere:

$P_{PVGU}(t)$ isIs the total power from the PVGU; $P_{PVI(1,2,3,4)}$represents the power from PVI 1,2,3, and 4, respectively.

The performance of the PV model is highly influenced by the weather conditions, particularly, the impact of temperature. Hence, five parameters $\alpha, \beta, \gamma, R_s, and\ a$are acquainted for withthe non-linear impacts of the fault condition. The expression for the maximum output power generated by the PV module P_{pv} [7] is given in Equation (2) as:

$$P_{pv}(t) = N_s N_p * \frac{\left[\frac{V_{oc}}{V_t} - \ln\frac{V_{oc}}{V_t} + 0.72\right]}{1 + \frac{V_{oc}}{V_t}} * \left(1 - \frac{R_s I_{sc}}{V_{oc}}\right) * I_{sco}\left(\frac{G}{G_o}\right)^{\alpha} * \frac{V_{oco}}{1 + \beta \ln\frac{G_o}{G}} * \left(\frac{T_o}{T}\right)^{\gamma} \quad (2)$$

$$V_t = \frac{aKT}{q} \quad (3)$$

Equation (3) represents the thermal voltage, 'a' is the ideality factor,

K is the Boltzmann constant,T is the temperature of the PV module, G is irradiance, and q is the charge of the electron. $N_s\ and\ N_p$ are the series and the parallel PV modules, respectively,

$R_s$is the series resonant, α represents the photocurrent factor, β is the PV dimensionless coefficient, and γ represents the non-linear factor.

In addition, V_{oc} and I_{sc} are the open-circuit voltage and short-circuit current of the PV module, respectively.

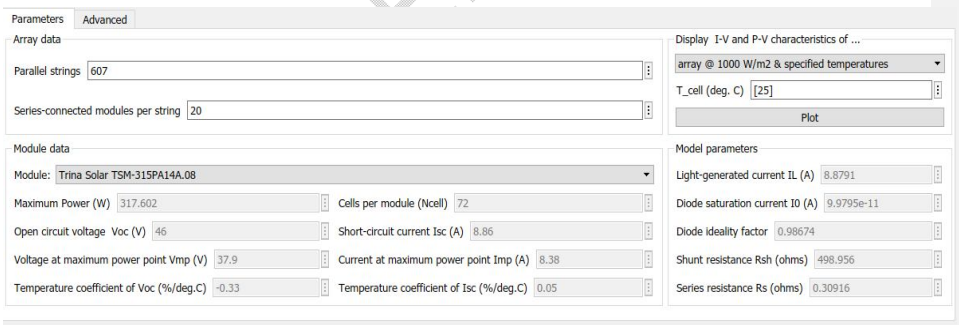

Figure 3: Parameters dialogue box of the PV Array

2.5 Diesel Generators (DGs)

The SHPP consists of three DGs all connected in parallel to step-up transformers. This connection is linked to 11 kV switchboard I as shown in Figure 1. DG 1 and DG 2 are rated 1,000 kVA each and connected to a 1.5 MVA step-up transformer;DG 3 is rated 1,500 kVA and connected to a 2.0 MVA step-up transformer, respectively.

2.6 Battery Stack

The battery stack is used to store the energy when the generated power is greater than the load demand. The battery power will be extracted when the generation cannot satisfy the

load requirements. Depending on the charging and discharging state, the current may be positive or negative. Losses may occur in both states, and hence, the state of charge (SoC) of the battery is expressed in Equation (4) [7].

$$SoC(t+1) = SoC(t) * \left(1 - \frac{\delta * \Delta t}{24}\right) + \frac{I_b(t) * \Delta t * \eta_b}{C_b} \quad (4)$$

~~where~~Where, δ represents the self-discharge rate, $I_b(t)$ is the current rate of the battery at time t,

$C_b$is the available capacity of the battery, and $\eta_b$is the efficiency of the battery.

The out- put power of the battery for the HRES is given in Equation (5) as:

$$P_b(t) = P_{PV}(t) + P_{DG}(t) - \frac{P_{acload}(t)}{\eta_{inv}} - P_{dcload} (5)$$

~~where~~ Where, η_{inv} is the inverter's efficiency, P_{acload} and P_{dcload} are the AC and DC loads respectively.

The limit of SoC of the battery stack is expressed in Equation (6):

$$SoC_{min} \leq SoC(t) \leq SoC_{max} (6)$$

2.7 Battery Bank Room (BBR)

The BBR ~~contains valve~~ valve-regulated ~~regulated~~ lead-acid (VRLA) batteries of 2V each in three rooms [11]. Connections from one battery to the other is accomplished via the series-parallel arrangement. Three hundred and sixty-six (366) cells form a string, there are eight strings of battery, and each string has a total of 1,098 batteries. The series connection of 366 cells in a string give a total voltage of 732V per string, the strings are terminated in parallel at the power conditioning system (PCS) unit in pairs, thus, making up a total of four PCS units. Each battery is rated at 4,100 Ah (Ampere-hour). The BBR sub-unit has a capacity of 24 MWhr (Megawatt hour), charging is based on SoC.

Connection: From the strings of batteries, the battery stack is connected to the PCS, hence, batteries are linked to the PCS. The PCS performs dual duties; it charges the batteries and also converts DC to AC. Four PCSs are installed/connected from the battery output.

PCS I and PCS II are connected in delta-star to a 2.5 MVA step-up transformer. PCS III and PCS IV are also connected in delta-star to another 2.5 MVA step-up transformer. These parallel arrangements are fed to the 11 kV bus bar where connections from the auxiliary unit, PVI and the DGs are linked. The complete Simulink model of the plant is shown in Figure 4.

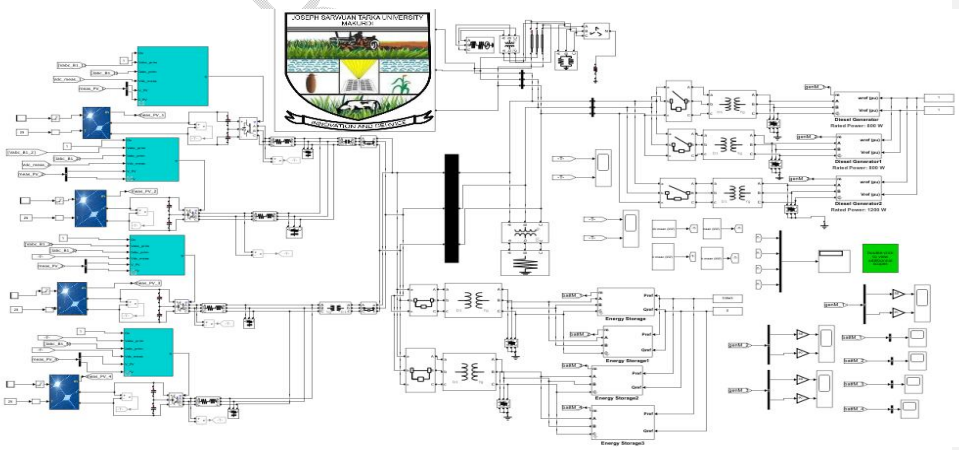

Figure 4: Simulink model of JOSTUM 3.5 MW SHPP

3.0 METHODS

3.1 Perturb and Observe (P and O) Algorithm

The P and O method for MPPT is proposed for this research, because of its simplicity; it possesses fewer measured parameters and can track maximum power point under varying irradiation and temperature quite accurately [9, 13].It can be seen in Figure 5 that, on right hand side of the P-V characteristics curve, as voltage decreases, power increases, while on left hand side of the characteristics curve, voltage increases as power increases. This is the main idea used in the p and o algorithm to track the maximum amount of power under all conditions.

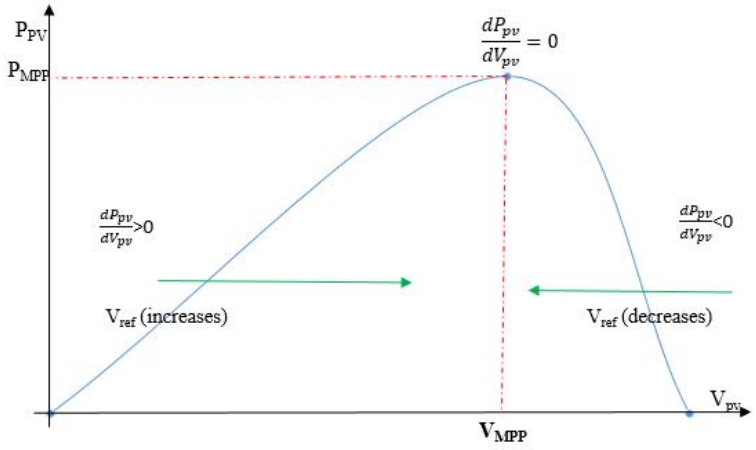

Figure 5: P-V Characteristics of PV panel [9]

3.1.1 Flowchart of the P and O algorithm

As seen in Figure 6, the P and O method is operated on the basis of periodical perturbations.

Formatted: Font: No underline, English (United Kingdom)

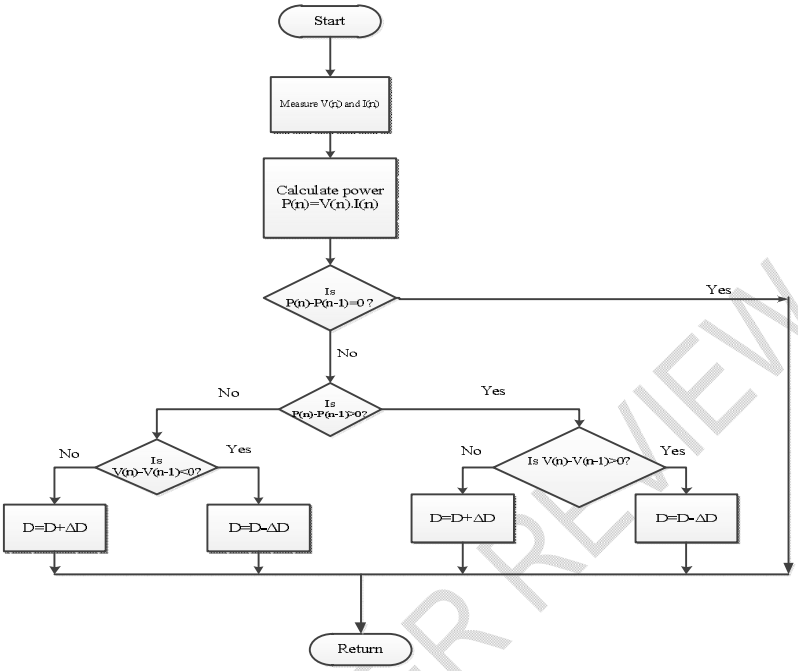

Figure 6: P and O algorithm flowchart

The first stage of P and O algorithm is to measure the initial PV voltage and current for the measurement of the initial power of PV system. If the difference of measured power is compared with previous power and the resultant is positive, the next perturbation increases in the same direction. In the case of a negative, the next perturbation is a decrease or reversal in the direction. The perturbation size in voltage (ΔV) or duty cycle (ΔD) is very small. The entire process is repeated periodically till the maximum power is observed from solar PV system [14]. However, the main drawback of this algorithm is the presence of oscillations around MPP.

3.1.2 Block diagram for MPPT of PV system

In order to increase the efficiency and to maintain the operating point at an optimum maximum power point of the PV power generation system, MPPT is used to track the MPP in its corresponding curve whenever there is a variation in the temperature or irradiation.

Formatted: No underline

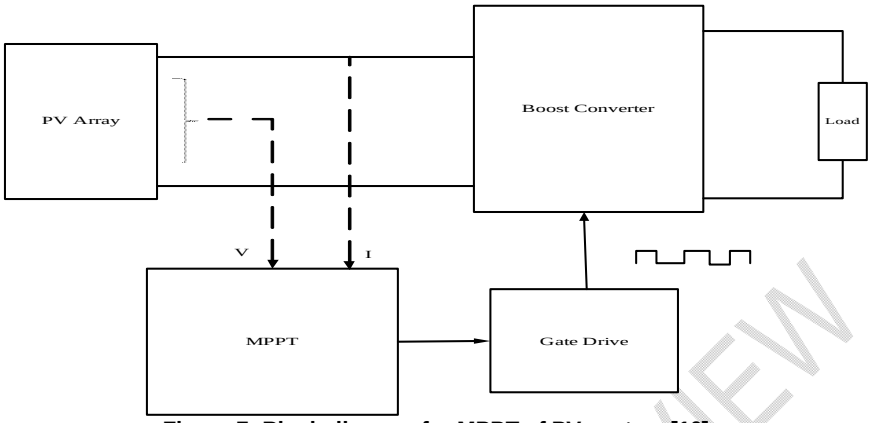

Figure 7: Block diagram for MPPT of PV system [10]

To keep maintaining this point at an optimum value, a power conditioner or a converter is added as an interface between the PV generator and the load. It extracts the maximum power from the source and transfers it to the load by stepping up (boost) or stepping down (buck) as per the requirement at the load side, the power transfer is carried out in accordance with the maximum power value by varying the on/off duty cycle of switch of the DC-DC converter [9, 13].

3.2 PVI Control Technique

The PVI does the job of power conversion from DC to AC. It is always on active state of MPPT; it extracts maximum amount of power for the modules under all conditions.

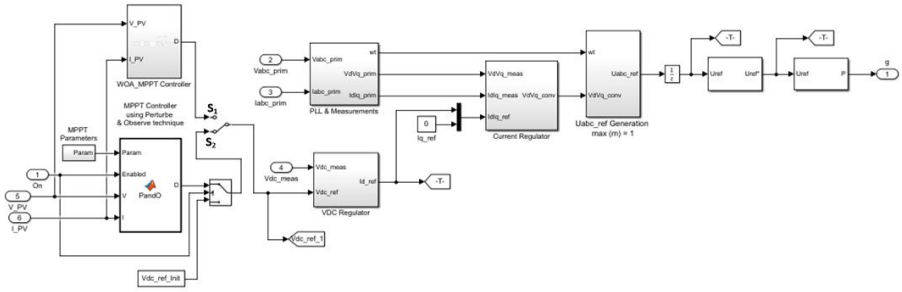

Figure 8: Simulink model of PVI control comprising of P and O-MPPT and WOA-MPPT based techniques

Two control techniques (algorithms) were tested during the simulation with the aid of a manual switch connected across the two controllers. These techniques are shown in Figure 8.

3.2.1 Maximum power point tracking (MPPT) controller

The MPPT controller is modelled based on the P and O/WOA as shown in Figure 8, such that when the toggle is S_2, the system is operating on P and O- MPPT technique, whereas when it is switched to S_1, the system is operating on WOA-based technique. In modelling the WOA-based MPPT controller, a MATLAB function block is used.

Formatted: No underline

3.3 WOA and its Application for MPPT; the proposed control technique

3.3.1 Overview of WOA

WOA is inspired from bubble-net hunting strategy of humpback whales [1]. The humpback whales dive deeply, create bubbles in a spiral shape around the prey, and swim to the surface during the ~~manoeuvre~~ maneuver. They usually attack the small fishes close to the surface [2]. The Humpback whale is the biggest of all whales and it has a special hunting mechanism of spiral bubble-net feeding. These whales hunt the school of ~~fishes~~ fishor krill on the surface by creating distinctive bubbles in a circular path.

Humpback whales ~~encircles~~ encirclethe prey during the hunt and the encircling behaviour can be mathematically modelled as[1],

$$\vec{D} = \left|\vec{C}.\vec{X^*}(t) - \vec{X}(t)\right| (7)$$

$$\vec{X}(t+1) = \vec{X^*}(t) - \vec{A}.\vec{D} \quad (8)$$

~~where~~ Where, $\vec{X^*}(t)$ is the whale's best position vector, which is updated in each iteration if there is a better solution, t represents the current iteration, $\vec{X}(t)$ is the prey position vector, $\vec{A}, \vec{D}$, and $\vec{C}$arethe coefficient vectors, which can be calculated as follows:

$$\vec{A} = 2\vec{a}.\vec{r} - \vec{a} \quad (9)$$

$$\vec{C} = 2.\vec{r} \quad (10)$$

~~where~~Where, $\vec{a}$ is linearly decreased from 2 to 0 over the course of iterations (in both exploration andexploitation phases) and $\vec{r}$ is a random vector in [0,1].

3.4 Application of WOA for MPPT

In this work, WOA is implemented as a direct control MPPT technique i.e., duty cycle control by taking the population of whales as duty ratios to reduce steady-state oscillations. Direct control MPPT decreases power loss and therefore improves the efficiency of the system. For each population of whales, i.e., duty ratios, the corresponding voltage and current are sensed by the controller, and output power is computed [10]. The main objective of optimal control is to determine control signals that will cause a process (plant) to satisfy some physical constraints and at the same time ~~extremize~~ optimise(~~maximize~~ maximiseor ~~minimize~~minimise) a chosen performance criterion (performance index or cost function) [12].

Here, MPPT is formulated as an objective function and it is represented as follows:

$$maximize\ P(d) > 0 \quad (11)$$

M~~m~~aximize P(d) subject to Equation (12),

$$d_{min} \leq d \leq d_{max} \quad (12)$$

~~where~~Where,$P$is PV output power, d is duty ratio,$d_{min}$is the minimum and $d_{max}$is the maximum limits of duty ratio i.e., 0.1 and 0.9, respectively. The block diagram for MPPT of PV system is depicted in Figure 7.

For MPPT, Equation (8) can be remodeled as

$$d_i(k+1) = d_i(k) - A.D \quad (13)$$

The objective function of WOA MPPT is formulated as

$$P(d_i^k) > P(d_i^{k-1}) \quad (14)$$

~~where~~Whereis the population of whales.

PV power is dependent on climatic conditions, for a change in solar irradiation of PV modules, the power output of PV array changes correspondingly and the proposed MPPT algorithm is reinitialized by sensing the change in PV output power using Equation (15).

$$\frac{P^k - P^{k-1}}{P^k} \geq 0.1 \quad (15)$$

3.4.1 Flowchart ofWOA-MPPT algorithm

The flow chart of the WOA is depicted in Figure 9, firstly, the voltage and current are measured and their values are used to calculate power,which is comparedwith the previous one

Formatted: No underline

Formatted: No underline

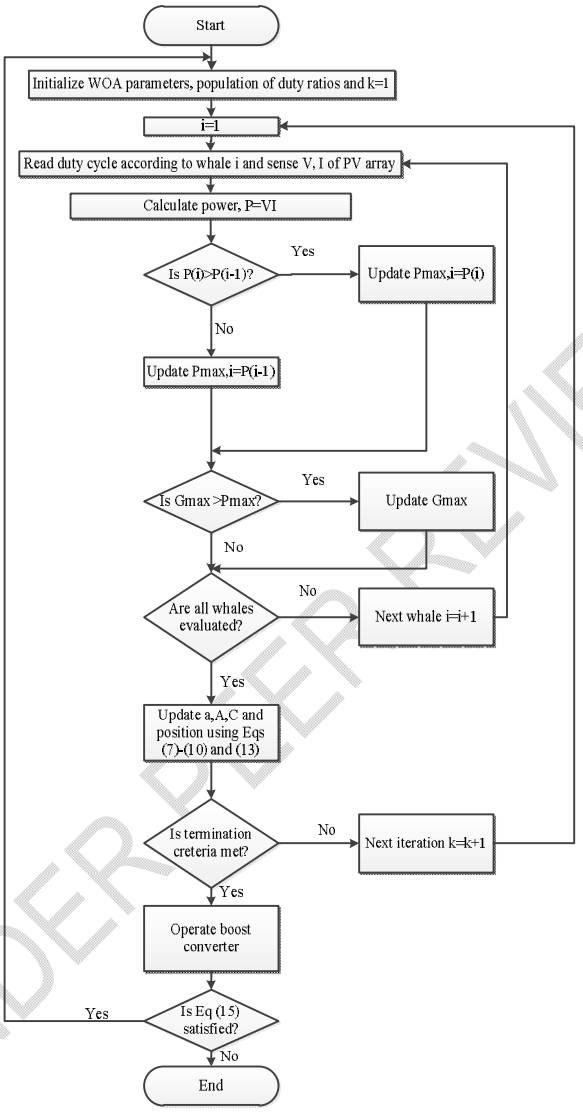

Figure 9: WOA-MPPT algorithm flowchart

and accordingly increases or decreases the voltage to locate the MPP by altering the duty cycle of the converter. The DC/DC converter is characterized by its duty cycle (d) that gives the ratio between the input and the output voltage when the conduction is continuous.

$$Duty\ cycle\ (d) = 1 - \left(\frac{input\ voltage}{output\ voltage}\right) \quad (16)$$

4. RESULTS AND DISCUSSION

This section presents the simulation results of the SHPP. ~~The energy~~ Energy management has been implemented using the WOA described in the previous section. In order to make an appropriate comparison of the different scenarios, the same inputs and system settings must be used. The model of the SHPP model is built using MATLAB/Simulink codes written in m-files, which are interfaced with the SHPP model to perform the optimization process. The system performance is evaluated and simulation results obtained from plots and scopes of the system and sub-systems are captured. Detailed results of the PV array under varying irradiances and temperatures, currents, voltage, and power of the PV array are presented. The results are illustrated in Figures 10-16.

The current-voltage (I-V) relation and power-voltage (P-V) relation of a single module at 25 degrees and varying solar irradiances are depicted in Figure 10, respectively. As it can be observed, the steady-states follow perfectly the optimal trajectories and are not affected by the solar irradiation and cell temperature variations. This leads to an important extraction of the available solar power and ~~an~~ improved performance of the system. The practical results demonstrate that PV system can be controlled perfectly by the proposed method. Figure 10 shows the I-V and P-V characteristics of a single PV module. At a standard irradiance of 1,000 W/m^2, the module produced a current of 8.83 A and a voltage of 37.9 V at the maxima point. The module extracted 1.776 A and 42.83 V at 200 W/m^2 irradiation. The P-V behaviour for a single module at MPP is 317 W, 37.9 V at 1,000 W/m^2, while at ~~a~~ lower irradiation of 200 W/m^2, the module tracked 62.03 W and 37.02 V at the maxima point. As shown in P-V characteristics, the point where the power is the highest is called the maximum power point (MPP), this power depends on the temperature and irradiation, also the load imposes its own characteristic which is generally different from the MPP.

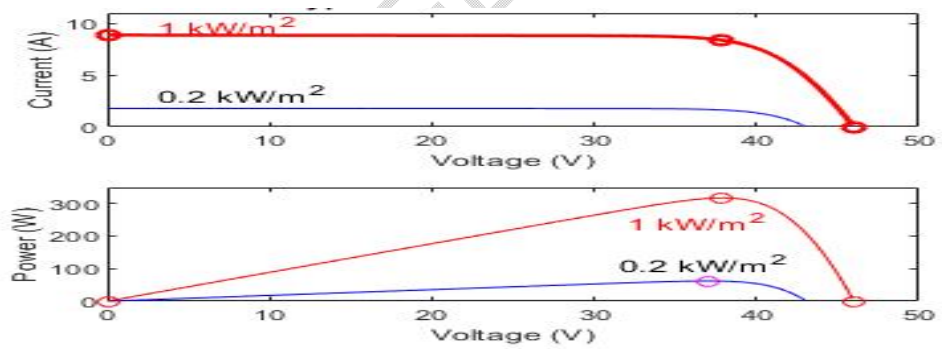

Figure 10: I-V relation and P-V relation of a single module at 25 degrees and varying solar irradiances.

Figure 11 shows the current-voltage (I-V) and power-voltage (P-V) characteristic of the array at 25^{o}C and specified irradiances. At 1,000 W/m^2, the array produced 5087 A and 758 V, technically speaking, the array gets ~~an~~ irradiation of 1,000 W/m^2 between 11 am and 3 pm, i.e., during sunny days (good days). During these periods, the array attracts a great amount of power which is used to run the plant and also for storage. At an irradiance of 200 W/m^2; which is during a period of low irradiance, the array tracked up to 1033 A and a voltage of 727.3 V. The low irradiance could be attributed to rainy or dull days. The maximum power and voltage achievable were 3.856 MW and 758 V at 1,000 W/m^2. At ~~a~~ lower solar irradiation of 200 W/m^2, 0.753 MW, and 740 V was tracked at the maximum point.

Comparatively, it can be seen that there is a drop in power, this is because of the drop in solar irradiation. An active power of 3.856 MW can conveniently run the plant and simultaneously be stored for usage during dull times.

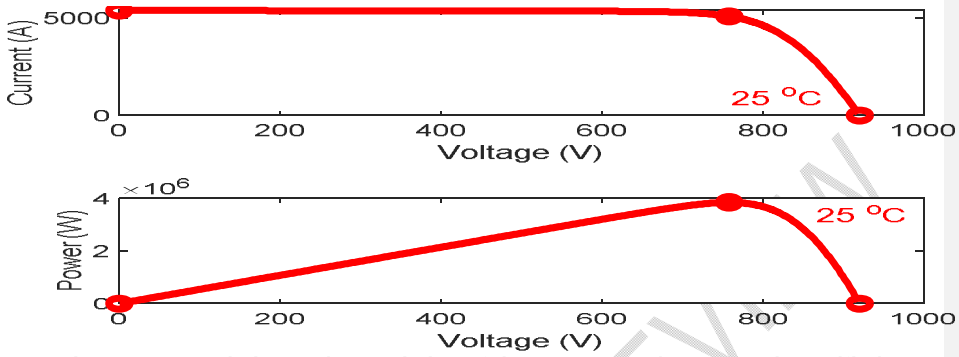

Figure 11: I-V relation and P-V relation of the array at 25 degrees and specified irradiance.

Figure 12 shows the I-V and P-V characteristics of an array at an irradiance of 1,000 W/m^2 and a temperature of 25^{o}C. It can be seen that 5087 A, 758 V, and 3.856 MW, 758 V were tracked, respectively. The main objective of an MPPT controller is to deal with the problems associated with the fluctuation and intermittency of renewable energy sources due to the change in weather conditions while EMS is used to optimize operations, ensure system's reliability, and provide power flow control in both standalone and grid-connected microgrids. With an output power of 3.856 MW, the plant through the EMS can schedule which source to take priority of the available load demand and allocate some percentage of power generated to the batteries for storage. The stored energy is used during periods of low or no irradiation till batteries reach the depth of discharge (DoD).

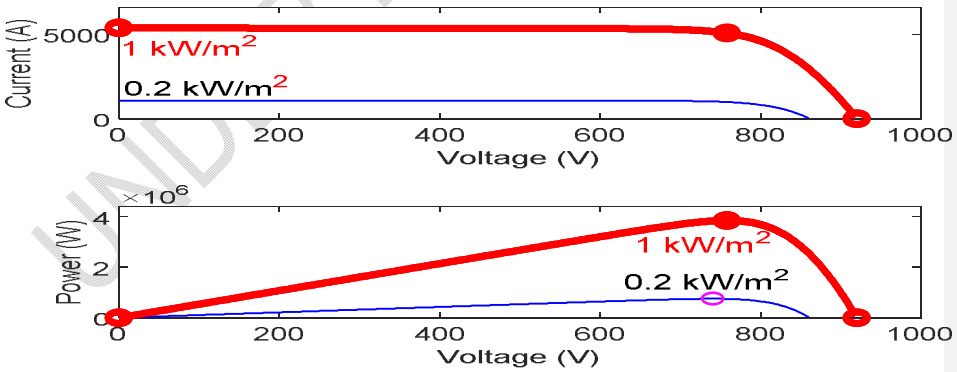

Figure 12: I-V and P-V characteristics of the array ~~at~~the specified temperature and varying solar irradiance.

It can be seen that~~,~~ solar irradiation varies proportionally with the corresponding values of current and voltage i.e., power, this can be obtained in F~~f~~igure 13 which depicts the relationship of voltage and power with respect to solar irradiance of the existing plant. In

Figure 14, the P and O MPPT algorithm is applied to the system. ~~Simulatio~~ The simulation was performed for 5 seconds at 1,000 W/m^2 and 200 W/m^2, respectively. Between 0.5 seconds and 1 second, solar irradiation dropped to 200 W/m^2. This shows that for V and P, the voltage dropped from 920 V to 820 V, while power also dropped from 2,300 kW to about 300 W within the same interval. As irradiation increases, the voltage rises back to 900 V with power also increasing back to 2,300 kW. The mean output power of the array was 2,300 kW which is greater than the output power of the array from the existing plant, which was 1,800 kW as shown in F~~f~~igure 13. To operate a PV array at the MPP, the DC/DC converter controlled by MPPT is inserted between the PV panel and the load [9]. The results show that the P and O MPPT controller having inputs of current and voltage from the array has stepped up the power through its duty cycle; which is its output. This duty cycle has boosted the converter in order to increase the output of the array to 2,300 kW. As shown in Figure 14, the MPPT is based on the conventional P and O algorithm. The command of boost converter alpha (α) is modified when the power increases or decreases as per solar irradiation.

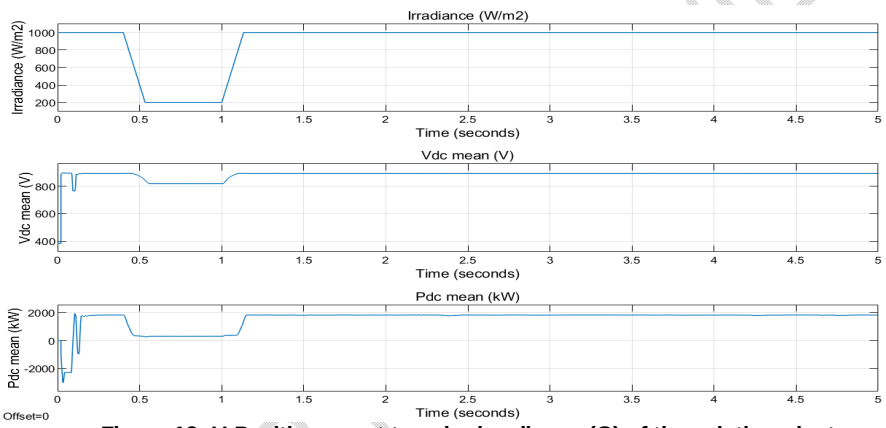

Figure 13: V-P with respect to solar irradiance (G) of the existing plant

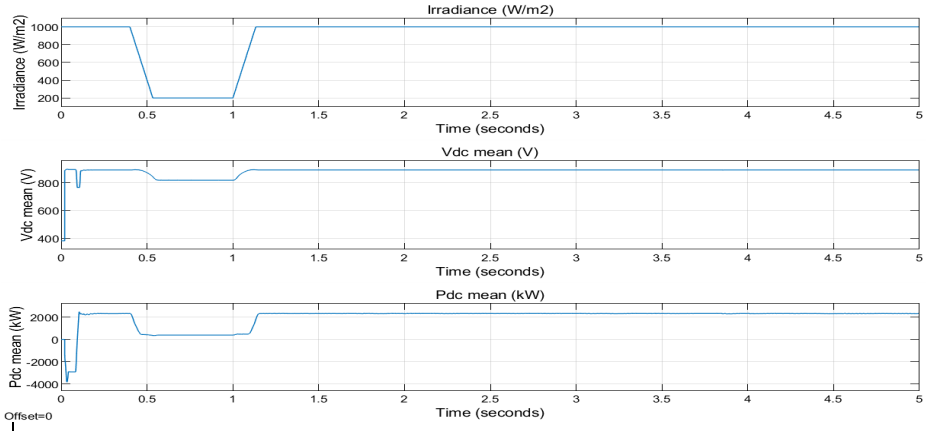

Figure 14: V-P with respect to solar irradiance (G) under P and O-based MPPT control technique.

In this study, the proposed WOA-based MPPT control is developed for MPPT control of the PV source. Based on the simulated results, the proposed method can efficiently track the maximum power under various weather conditions and minimize steady-state oscillations occurring at MPP. Figure 15 illustrates the performance of the dynamic response of the PV array's voltage and power with respect to irradiances when the WOA-based MPPT algorithm was applied to the system. The generated voltage of the array varies between the time intervals of 0.5 second to 1 second over a simulation time of 5 seconds, while variation in voltage occurred due to drop in solar irradiation from 1,000 W/m^2 to 200 W/m^2. A stable voltage of about 900 V was maintained throughout the simulation when irradiation was at 1,000 W/m^2. Similarly, between 0.5 seconds and 1 second, the output power dropped because of little or no solar irradiation. Solar irradiation is directly proportional to the power of the array, as seen in Figure 15, with the increment in irradiation giving rise to increment in output power of the system. The proposed technique boosted the DC/DC converter to produce about 2,800 kW. As earlier mentioned, the WOA-based MPPT controller greatly minimized power loss around the MPP, which is largely caused by oscillations. Results of the simulation have proven this claim, hence a difference of 1000 kW is seen between the existing plant and the WOA-based controller, and up to 500 kW difference between P and O and WOA-based MPPT controller. Figure 16 illustrates the comparison of the existing plant, P and O MPPT based and WOA-based MPPT controllers with respect to the output power of the PV array. This shows the superiority of the WOA- based MPPT control technique over the P and O MPPT based control technique and the existing plant.

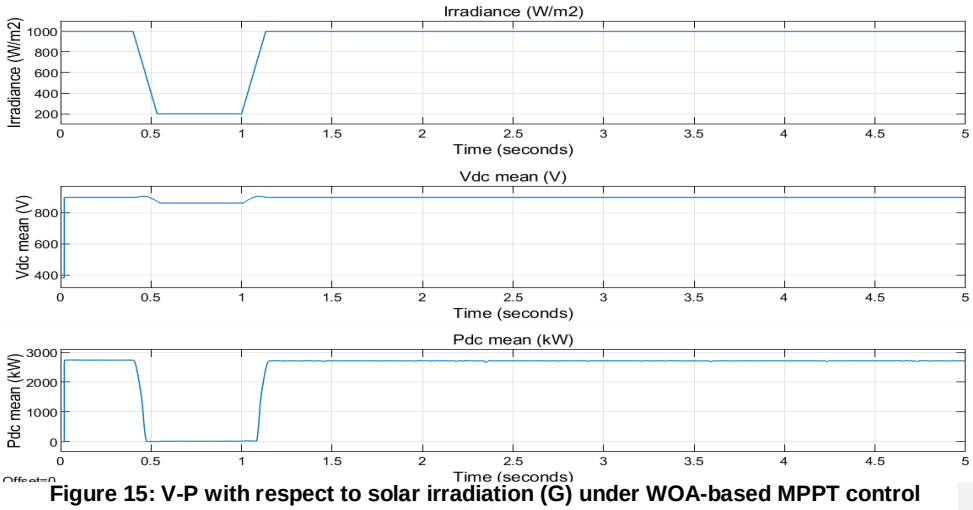

Figure 15: V-P with respect to solar irradiation (G) under WOA-based MPPT control technique.

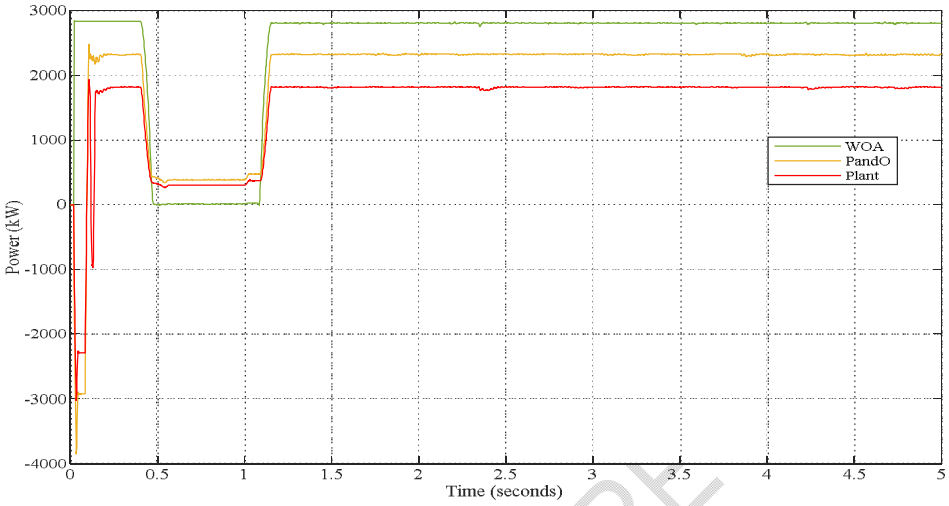

Figure 16: Comparism of WOA, P and O, and the existing plant with respect to PV array's output power.

5. CONCLUSION

An optimal control technique; WOA-based MPPT control has been proposed for the control of the SHPP. The proposed system consists of an MPPT controller; which receives inputs of current and voltage from the PV array, a gate drive; which is inputted by the duty cycle, and a boost converter; which outputs a higher power to the load side. The WOA algorithm optimally improves the gains of the MPPT controller in light of maximum efficiency i.e., objective function P(d) which is the output power of the array in terms of duty cycle (d). The proposed technique is carried out in the MATLAB/Simulink environment. The simulation results are analyzed under varying solar irradiations and the power i.e., current and voltage characteristics with respect to varying irradiance are displayed. The simulation results show the predominance of the proposed technique in comparison with the existing technique. WOA-based MPPT has 55.56% efficiency while the P and O MPPT-based has 27.78% efficiency. Similarly, 1.8 MW is 51% of 3.5 MW. The WOA-based MPPT controller effectively delivered 2.8 MW output, i.e., 80% of the rated capacity. For future studies, research should be carried out on the power conversion devices; the PVI and PCS should be reconfigured and incorporated as a single unit, as this would reduce the installation cost and space. Further study on the optimal control of battery charging for the control strategies of batteries should be explored to deal with the control problems of continuous state space and actions.

COMPETING INTERESTS

Authors have declared that no competing interests exist.

REFERENCES

1. Mirjalili S and Lewis A. The whale optimization algorithm. Advances in Engineering Software.2016; 95(18): 1–8.
2. Hasanien HM. Whale optimization algorithm for automatic generation control of interconnected modern power systems including renewable energy sources. Institute of Engineering and Technology (IET). 2017; 12(5): 1-7.

3. Gajewski P and Pieńkowski K. Control of the hybrid renewable energy System with wind turbine , photovoltaic panels and Battery energy storage. Energies. 2021; 14(6): 2-11.
4. Reddy SS. Optimal power flow with renewable energy resources including storage. Electrical Engineering. 2017; 99(2): 685–695.
5. Reddy PDP, Reddy VCV and Manohar TG. Whale optimization algorithm for optimal sizing of renewable resources for loss reduction in distribution systems. Renewables,2017: 1-5.
6. Reddy SS. Multi-objective optimal power flow for a thermal-wind-solar power system. Journal of Green Engineering. 2018; 7(4): 3–16.
7. Venkatesan K and Govindarajan U. Optimal power flow control of hybrid renewable energy system with energy storage: A WOANN strategy. Journal of Renewable and Sustainable Energy (JRSE). 2019; 11(1):1-5.
8. Mossad MI. Whale optimization algorithms-based PI controllers of STATCOM for renewable hybrid power system. World Journal of Modelling and Simulation. 2020; 16(1): 2-10.
9. Guiza D, Ounnas D, Soufi Y and Maamri M. Implementation of perturb and observe-based MPPT algorithm for PV system. International Conference on Sustainable Renewable Energy Systems and Applications (ICSRESA); Tebessa Algeria, Februay 2019: 2-5.
10. Santhan CHK and Rao RS. A novel global MPP tracking of photovoltaic system based on WOA. International Journal of Renewable Energy Development. 2016; 5(3): 225-232.
11. Akuhwa TD, Udenze IP and Adzembe IJ. Planning and installation of 3.5 Megawatts off grid solar hybrid power plant: A case study of the Joseph Sarwuan Tarka University Makurdi. International Journal of Advances in Scientific Research and Engineering (IJASRE). 2022; 8(1): 1-7.
12. Desineni SN. Optimal control systems. Pocatello, Idaho U.S.A. CRC Press; 2002.
13. Saad M, Abdelaziz EG, Souad S, Aziz D and Abdulaziz G. Proposal and implentation of a novel perturb and observe algorithm using embedded software. 3rd IEEE International Renewable and Sustainable Energy Conference, Marrakech, Morocco. 2015: 1-5.
14. Maniraj B and Peer FA. PV output power enhancement using whale optimization algorithm under normal and shading conditions. International Journal of Renewable Energy Research (IJRER). 2020; 10(3): 2-6.